

CROFT: A scalable three-dimensional parallel Fast Fourier Transform (FFT) implementation for High Performance Clusters

Vivek Gavane^{1,*}, Supriya Prabhugawankar¹, Shivam Garg, Archana Achalere, Rajendra Joshi*

HPC-Medical and Bioinformatics Applications Group, Centre for Development of Advanced Computing(C-DAC), C-DAC Innovation Park, Pashan, Pune-411008, India.

Abstract

The FFT of three-dimensional (3D) input data is an important computational kernel of numerical simulations and is widely used in High Performance Computing (HPC) codes running on large number of processors. Although the efficient parallelization of 3D FFT has been largely investigated over the last few decades, performance and scalability of parallel 3D FFT methods on new generation hardware architecture for HPC is a major challenge. Looking at upcoming exascale cluster architectures, the conventional parallel 3D FFT calculations on HPC needs improvement for better performance.

In this paper, we present C-DAC's three-dimensional Fast Fourier Transform (CROFT) library which implements three-dimensional parallel FFT using pencil decomposition. To exploit the multithreading capabilities of hardware without affecting performance, CROFT is designed to use hybrid programming model of OpenMP and MPI. CROFT implementation has a feature of overlapping compute and memory-I/O with MPI communication. Depending on the number of processes used, CROFT shows performance improvement of about 51%–42% as compared to FFTW3 library.

Keywords: 3D FFT, pencil decomposition, 2D decomposition, parallel FFT.

*Corresponding author

Email addresses: vivekg@cdac.in (Vivek Gavane), rajendra@cdac.in (Rajendra Joshi)

¹Vivek Gavane and Supriya Prabhugawankar should be regarded as joint first authors

1. Introduction

Fast Fourier Transform (FFT) is an extensively used algorithm which calculates the Discrete Fourier Transform (DFT) of N complex points. Discrete Fourier Transform is the most fundamental mathematical tool applied to time series and waveform analysis in signal processing, applied mathematics, spectral analysis, control processing etc [1]. With the famous divide and conquer algorithm by Cooley and Tukey [2], FFT algorithm reduced the time complexity of naive implementation of DFT from $O(n^2)$ to $O(n \log n)$ for serial computation. It also opened up active area for parallel implementation of FFT algorithms, depending on data size and machine architecture. Fast Fourier Transform as a numerical tool, has been extensively used across wide disciplines of science and engineering. For example, its application ranges from turbulence simulations, computational chemistry and biology, gravitational interactions, cardiac electrophysiology, acoustic, seismic and electromagnetic scattering, image processing and many other areas [3], [4],[5], [6], [7].

In most of these applications, FFT is applied on large data sets with multiple dimensions. This makes FFT calculations computationally intensive, and parallel FFT involves data distribution and collective communication. Therefore, a lot of efforts on research and development in parallelization of FFT, especially on 3D FFT, have been carried out for a variety of domain specific applications. With modern day HPC environment, where large number of processors are available, scalability and performance of 3D FFT is a major challenge. Parallelization of FFT algorithm can be broadly categorized as distributed FFT and transpose-based algorithms [8] [9]. In order to utilize the maximum number of processors in modern day HPC machines, transpose-based algorithms have been predominantly used in many parallel 3D FFT codes.

Parallel FFT on multidimensional data can be performed as a sequence of one-dimensional transforms along each dimension. This demands data distribution, that involves lot of communication across the processors and hence,

prevents the efficient usage of large number of processors for a given data size. The efficiently scaled implementation of parallel 3D FFT on new generation HPC hardware is one of the grand challenges in scientific computing. Since last two decades lots of efforts have been made to resolve this issue using different strategies. Therefore, many parallel open source FFT libraries exist and have been efficiently used in academia and industry as well. FFTW (Fastest Fourier Transform from West)[11], PFFT (Parallel FFT) [12], P3DFFT (Parallel Three-Dimensional Fast Fourier Transforms)[13] and 2DECOMP&FFT [23] are few such libraries. Most of the conventional parallel 3D FFT libraries are based on 1D or slab decomposition method, which limits scaling only up to the largest dimension of multidimensional data. While using pencil or 2D decomposition, scalability of 3D FFT has been improved in libraries like P3DFFT and 2DECOMP&FFT. All of these libraries use MPI for message passing on a distributed cluster for parallel FFT calculations. On the other hand, hardware reconfiguration techniques and accelerators have also been used to obtain performance of 3D FFT [16],[17],[18]. Similarly, 3D parallel FFT libraries like AccFFT have been developed to achieve scalability and performance on both CPU and GPU architectures [15]. Recently, to improve the scalability of 3D parallel FFT, use of non-blocking MPI call has been reported[19]. Also combination of OpenMP and MPI has been used on HPC to speed up 3D FFT parallel calculations [20].

In this paper, we present CROFT library to calculate 3D parallel FFT using MPI and OpenMP hybrid programming model. CROFT's parallel strategy is designed and implemented for performance and scalability on large multicore clusters. In upcoming exascale clusters there is an increase in the total amount of memory per node and improvement in the operating frequency of main memory. High bandwidth and low latency networks are being designed for scalability of applications. To exploit the improvement in technology, this paper presents application of hybrid programming model comprising OpenMP and MPI having overlap of compute and memory-I/O with MPI communication. CROFT has demonstrated performance improvement of approximately 42% to 51% with

varying number of processes as compared to popularly used FFTW3 library.

2. Background and Implementation of parallel 3D FFT

2.1. Multidimensional FFT

The forward DFT of a three-dimensional complex input array $X = \{X(0 : N_x - 1, 0 : N_y - 1, 0 : N_z - 1)\}$ to a complex three-dimensional output array $Y = \{Y(0 : N_x - 1, 0 : N_y - 1, 0 : N_z - 1)\}$ is defined as [21],

$$Y(k_x, k_y, k_z) = \sum_{j_x=0}^{N_x-1} \sum_{j_y=0}^{N_y-1} \sum_{j_z=0}^{N_z-1} X(j_x, j_y, j_z) E \quad (1)$$

where, $E = e^{-2\pi i \left(\frac{k_x j_x}{N_x} + \frac{k_y j_y}{N_y} + \frac{k_z j_z}{N_z} \right)}$ and

$$0 \leq k_x < N_x,$$

$$0 \leq k_y < N_y,$$

$$0 \leq k_z < N_z$$

The corresponding backward DFT using the same definitions is defined as [21],

$$X(j_x, j_y, j_z) = \frac{1}{N_x N_y N_z} \sum_{k_x=0}^{N_x-1} \sum_{k_y=0}^{N_y-1} \sum_{k_z=0}^{N_z-1} Y(k_x, k_y, k_z) E \quad (2)$$

where, $E = e^{2\pi i \left(\frac{k_x j_x}{N_x} + \frac{k_y j_y}{N_y} + \frac{k_z j_z}{N_z} \right)}$ and

$$0 \leq j_x < N_x,$$

$$0 \leq j_y < N_y,$$

$$0 \leq j_z < N_z$$

(3)

For parallelization of 3D FFT, the 3D input matrix data can be decomposed and distributed amongst the processes [21]. To perform 3D FFT we have to take 1D FFT, along each dimension. This can be achieved using the serial 1D FFT as the building block.

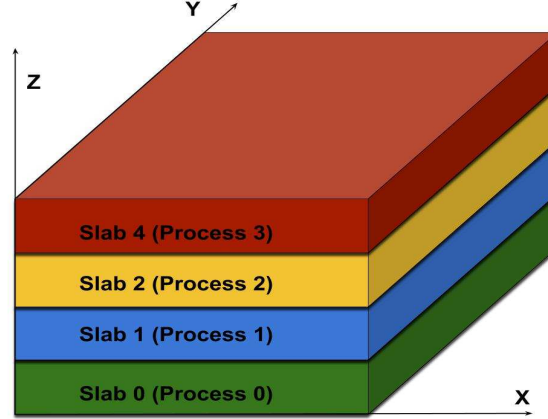


Figure 1: Slab or 1D decomposition technique for parallelization.

2.2. Decomposition techniques

There are three main data decomposition techniques available. These are 1) slab or 1D decomposition [8], 2) pencil or 2D decomposition [24] and 3) cell or 3D decomposition [25].

2.2.1. Slab Decomposition

In this approach 3D input matrix is decomposed along any one dimension resulting in multiple slabs which are given to different processes for further computations. For example, if input matrix has dimension $N_x \times N_y \times N_z$, and any one axis, say Z is chosen for decomposition, then the distributed input with every process will be,

$$N_x \times N_y \times \frac{N_z}{P_z} \quad (4)$$

where, $P = P_z =$ Number of processes along Z axis.

As data along the X and Y is contiguous in memory, we can either take 2D FFT transform or separately take 1D FFT along both the axes locally. These local transforms do not involve any kind of communication between the processes. After 2D transform along the X and Y dimensions, we have to take a

global transpose of the data and then perform 1D FFT along the Z axis. This global transpose is required to make the third dimension locally available on the processes and involves communication between the processes to exchange data. The scalability of the slab decomposition is limited by the number of slabs that can be created along a single dimension of the 3D matrix. In this case, the maximum number of processes that can be used is $P_{max} = N_z$. Thus, this technique is not suitable when large number of processors are available. Slab decomposition is used by many parallel 3D FFT libraries e.g. FFTW3 [11] and problem-specific applications e.g. molecular dynamics software GROMACS [28].

2.2.2. Pencil Decomposition

In this approach 3D input matrix is decomposed along two dimensions which forms a shape of pencil. Number of pencils generated are equal to the number of processes to be spawned. For example, if input 3D matrix has dimension $N_x \times N_y \times N_z$, then take any two dimensions for decomposition say Y and Z . The distributed input with every process will be,

$$N_x \times \frac{N_y}{P_y} \times \frac{N_z}{P_z} \tag{5}$$

where

$$\begin{aligned} P_y &= \text{Number of processes along } Y \text{ axis,} \\ P_z &= \text{Number of processes along } Z \text{ axis, and} \\ P &= P_y \times P_z \text{ is the total number of available processes.} \end{aligned} \tag{6}$$

The scaling limitation of 1D decomposition technique can be overcome by using a 2D decomposition technique. Here, maximum number of processes that can be used are $P_{max} = N_y \times N_z$ which is greater than that of slab decomposition.

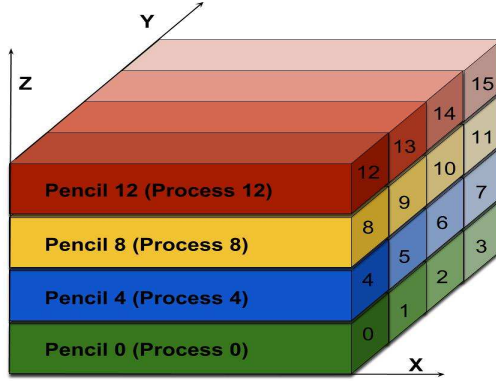


Figure 2: Pencil or 2D decomposition technique for parallelization.

2.2.3. Cell decomposition

In this approach 3D input matrix is decomposed along all three dimensions to form small cuboidal sub-matrices of data, called cells. Number of cells generated are equal to number of processes to be spawned. For example, if input 3D matrix has dimension $N_x \times N_y \times N_z$, then distributed input with every process will be,

$$\frac{N_x}{P_x} \times \frac{N_y}{P_y} \times \frac{N_z}{P_z} \quad (7)$$

where

P_x = Number of processes along X axis,

P_y = Number of processes along Y axis,

P_z = Number of processes along Z axis, and

$$P = P_x \times P_y \times P_z$$

is the total number of available processes.

For calculation of 3D FFT using this approach, we can use large number of processors, but computation becomes complex and involves huge amount of communication and hence is rarely used.

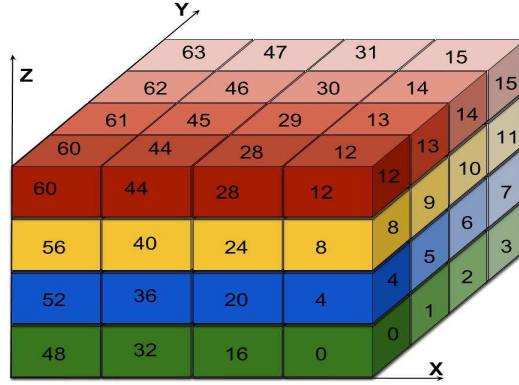


Figure 3: Cell or 3D decomposition technique for parallelization.

3. Related Work

To perform parallel 3D FFT, different open source libraries such as FFTW3, P3DFFT, and 2DECOMP&FFT are available. FFTW3 uses slab decomposition, whereas P3DFFT and 2DECOMP&FFT use pencil decomposition to distribute the data in parallel environment.

3.1. FFTW3

FFTW3 is a widely used free-software library that computes the Discrete Fourier Transform (DFT) and its various special cases [11], [26]. It is a C subroutine library for computing the DFT in one or more dimensions of arbitrary input size, and works on both real and complex data. It also works on even/odd data, i.e. the discrete cosine/sine transforms or DCT/DST respectively[26]. The latest official release of FFTW3 is version 3.3.8. Version 3.3 introduced support for AVX x86 extensions, a distributed-memory implementation on top of MPI, and a Fortran 2003 API [26]. This version is used for comparative study and serial 1D FFT calculations. FFTW3 uses slab decomposition and therefore its scaling is limited to $P_{max} \leq N$ where, P_{max} is maximum number of processors and N is linear problem size.

3.2. P3DFFT

Parallel Three-Dimensional Fast Fourier Transforms, dubbed P3DFFT is a library for large-scale computer simulations on parallel platforms [13]. P3DFFT is written in Fortran and is optimized for parallel performance. It uses Message Passing Interface (MPI) for interprocessor communication, and from v.2.7.5 onwards P3DFFT provides a multi-threading option for hybrid MPI/OpenMP implementation.

This library uses 2D or pencil decomposition to overcome an important scalability limitation which is known to be inherent in FFT libraries based on 1D (or slab) decomposition [27]. The number of processors/tasks used can be as large as $P_{max} = N_y \times N_z$, where N_y and N_z are input matrix sizes along the Y and Z dimensions respectively.

3.3. 2DECOMP&FFT

2DECOMP&FFT [23] library written in Fortran uses 2D or pencil decomposition for data distribution on distributed-memory platforms. It is one of the scalable and efficient distributed Fast Fourier Transform modules that supports three-dimensional FFT and includes both complex-to-complex and real-to-complex/complex-to-real transforms. The maximum number of processors/tasks that can be used are $P_{max} = N_y \times N_z$, where N_y and N_z are input matrix sizes along the Y and Z dimensions respectively.

4. Proposed Method

CROFT is a parallel three-dimensional Fast Fourier Transform library implementation for distributed clusters. We have used a general algorithm which is based on pencil decomposition for data distribution. It is implemented using hybrid programming and is based on the strategy of overlapping compute and communication operations. Three-dimensional FFT is obtained by calculating 1D FFT along all the three dimensions of the input data. CROFT uses 1D FFT routine from FFTW3 library to calculate the FFT along each dimension.

4.1. Algorithm

The algorithm requires 2^p processes which are arranged as a two dimensional matrix. Processes in each row form row-communicator and processes in each column form column-communicator resulting in multiple row and column communicators as seen in figure 5. The algorithm requires each process to have its part of data. For the sake of understanding, it is assumed that the data is aligned along the X dimension. The data is decomposed along the Y and Z dimensions to form multiple pencils, which are aligned along the X dimension as seen in figure 4(a). The number of pencils would be equal to the number of processes, where, one pencil is assigned to each process. The steps followed by CROFT are given below.

Steps:

1. Compute 1-D FFT along the X dimension for all processes.
2. Pack the 1-D array data into a buffer in preparation for all-to-all communication.
3. For all column communicators, perform all-to-all communication between all processes in a column communicator.
4. Rearrange the received data into the 1-D array with the new memory layout such that elements on the Y dimension are adjacent in memory.
5. Compute 1-D FFT along the Y dimension.
6. Pack the 1-D array data into a buffer in preparation for all-to-all communication.
7. For all row communicators, perform all-to-all communication for each process in a row communicator.
8. Rearrange the received data into the 1-D array with new memory layout such that the elements on the Z dimension are adjacent in memory.
9. Compute 1-D FFT along the Z dimension.

4.2. Algorithm Explanation

Initially, the data is distributed to each process as a pencil in which the data is aligned along the X axis. Each process now computes 1D FFT along the X

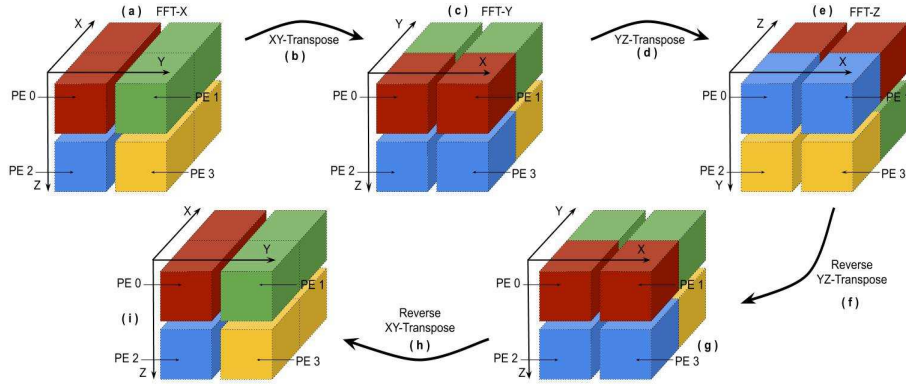


Figure 4: Steps involved in computing 3D parallel FFT. Pencil image indicates 1D FFT calculations along a dimension and arrow between two images indicates transpose.

axis and saves the result in 1D array. To compute FFT along the Y axis, XY transpose is performed so that data along the Y axis becomes contiguous. This is achieved using step 2, 3 and 4 of the algorithm. The 1-D array data is packed into a buffer, such that the buffer is filled with data which is to be communicated, followed by all-to-all communication in the column communicator. Both these operations, packing and MPI all-to-all communication have been overlapped. After the completion of communication, the data is unpacked and rearranged in the memory, so that the data along the Y axis would be contiguous. Now, the 1D FFT is computed along the Y dimension and the result is saved in 1D array. The FFT along the Z axis is computed, by performing YZ transpose, so that data along the Z axis would be contiguous as per the steps 6, 7 and 8. This is followed by the overlap of the operations involving packing of data with MPI all-to-all communication in row communicator. After the completion of communication, the date is unpacked and rearranged in memory so that the data along Z axis would be contiguous. Now, 1-D FFT is computed along the Z dimension and the result is saved in 1D array. To get the same data layout as initial, YZ and XY transpose are performed.

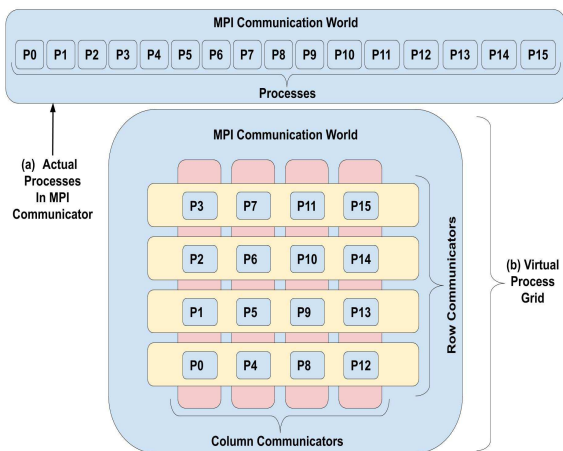


Figure 5: 2D virtual communication grid formed by processes in 2D or pencil decomposition

5. Implementation and verification

The above mentioned algorithm (Section 4.1) is implemented in CROFT library to calculate parallel 3D FFT using pencil decomposition. The implementation is done in C using MPI+OpenMP hybrid programming model for double precision complex data. This implementation considers the dimensions of actual 3D matrix as N_x , N_y and N_z , where $N_x = N_y = N_z$ and is equal to 2^n for any integer n . We have discussed the implementation of forward transform in this paper. The backward transform can be obtained by reversing the steps in the algorithm.

5.1. Parallelization and optimization

Message Passing Interface (MPI) library is used to communicate across the processes in a distributed cluster. The total number of processes are virtually arranged in 2D virtual communication grid as shown in figure 5, with P_y as the number of processes along the Y axis and P_z as the number of processes along the Z axis.

Initially, as the data is contiguous along the X axis, each process first performs a 1D FFT along it. For all the nodes to have the Y dimension locally

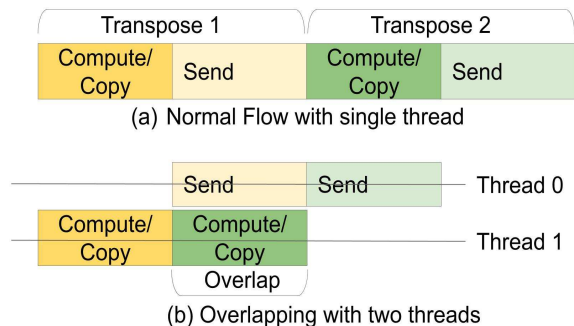


Figure 6: Overlapping of data copy and communication operations.

available, a global transpose is required. It then takes global transpose and performs 1D FFT along the Y axis. At this stage, to swap the X and Y axis, all-to-all communication between processes within the same row of the virtual communication grid takes place. It again performs global transpose and 1D FFT along the Z axis. This global transpose is required for the nodes to have the Z dimension locally available. Here, all-to-all communication between processes within the same column of the virtual communication grid is required to swap the data along the Y and Z axis.

OpenMP is used for overlapping compute and memory I/O with communication operations. The implementation uses two threads as seen in figure 6(b) with one thread dedicated for MPI communication. While one thread is executing the application, if communication is demanded, it is handled by the other thread. Here, we define an iteration parameter K to handle the trade-off between size of overlapping computation and memory I/O chunk with the communication calls. With a small value of K , we can overlap large chunk of compute and memory I/O operations with the communication calls, which results into less communication overhead. If the value of parameter K gets large, we can overlap smaller chunks of compute and memory I/O operations with the communication, which results into more number of communication calls. Thus we should find an optimum value of $K \geq 1$ to achieve high performance.

For optimizing the code execution, various techniques such as function inlin-

ing and vectorization is used wherever possible. For checking the performance with different implementation approaches, code was implemented for various combinations of compute and communication options. These options include:

Option 1 : without overlap of compute and communication while using multiple FFTW3 plans for calculating 1D FFTs;

Option 2: without overlap of compute and communication while using single FFTW3 plan for calculating multiple 1D FFTs;

Option 3 : with overlap of compute and communication while using multiple FFTW3 plans for calculating 1D FFTs;

Option 4: with overlap of compute and communication while using single FFTW3 plan for calculating multiple 1D FFTs.

However, as option 4 has been observed to perform better on large data and large number of processors, CROFT library is implemented using option 4 with the value of K fixed as 2.

5.2. Forward transform implementation

Forward transform is computed after data is divided in number of pencils as seen in figure 4(a). Every process will get its own chunk of 3D pencil data ($N_x, N_y/P_y, N_z/P_z$ according to pencil decomposition) as a 1D input array. Each process executes the above given algorithm with the help of two OpenMP threads which are spawned after first step. The thread with thread Id 0 is used for MPI communication and the thread with thread Id 1 is used for packing the data into buffer and performing 1D FFT as seen in figure 6(b). Two threads run simultaneously and achieve overlapping of computation and memory I/O with all-to-all communication, i.e step 2 and step 3 of the algorithm are successfully overlapped. After the communication the data is unpacked and FFT along the Y direction is computed. Once again packing of data and all-to-all communication steps are overlapped in preparation for the FFT along the last dimension. Then the data received after communication is unpacked and FFT along the Z direction is computed. To get the same data layout as initial, we

again perform YZ and XY transpose respectively and use overlapping of data packing with MPI all-to-all communication.

5.3. Verification of code

3D parallel FFT using pencil decomposition requires MPI all-to-all communication and many data copy operations within local memory for rearranging the data. Therefore, it is necessary to verify the result after every step. For verification purpose, we first implemented routines to print the results and verified the generated output data with the desired output for the given input. Secondly, we have taken backward FFT to get back the original input. Since, we did not perform any manipulations while using normalization factor, output of backward transform is same as input applied. Finally, to check the correctness, we tested the results obtained by CROFT library against the results from FFTW3 library for double precision complex input. The output was found to be exactly the same.

6. Discussion and Results

6.1. Benchmarking details

CROFT was benchmarked against 3D FFT API from FFTW3v3.3.8 on Param Bioblaze cluster and Sangam Lab cluster which are internal clusters in C-DAC. The Param Bioblaze cluster is a blade based cluster with two chassis which are interconnected with an external 56 Gbps Mellanox FDR IB switch. Each chassis contains 16 dual socket blade servers connected through internal FDR IB switch. Each blade server has two 8 core Intel sandy bridge processors and 64 GB RAM. So, the number of cores in Param Bioblaze cluster accumulates to a total 512 compute cores.

The input data used for the benchmarking purpose was the 3D matrix of double precision complex numbers. As the number of cores and RAM per core were limited, the first benchmark was done with the smaller 3D matrix of size $128 \times 128 \times 128$, and another benchmark with the larger 3D matrix of size $1024 \times 1024 \times 1024$.

6.1.1. Time measurements

The timing information is collected for benchmarking purpose using MPI_Wtime API. The starting timestamp is collected just before calling the 3D FFT API of CROFT and FFTW3 library functions. The processes are synchronized at a global barrier to avoid distortion of the time before collecting the initial timestamps. Another timestamp is collected just after the 3D FFT API execution is completed. The difference between the two timestamps is considered as the execution time required for the process to perform 3D FFT. We then get the minimum and maximum execution time taken by the processes onto processor 0 using a global reduction with MPI_MAX and MPI_MIN options. The time obtained from MPI_MAX reduction is considered as the wall time required by the 3D FFT library function. To get the final wall time, multiple runs of application are done and the best timings are selected.

6.2. Results

Benchmarking runs were performed on parallel 3D API of FFTW3 and all the implemented options as discussed in Section 5.1.

Table 1 shows the benchmarking timings on Param Bioblaze cluster with fill up allocation, i.e. all cores on a node are used before spawning to the next node, and table 2 shows the timings obtained by custom layout of processes. For the 3D matrix of size $128 \times 128 \times 128$, FFTW3 code can use up to 128 cores due to the use of slab decomposition and it is evident from the time taken by FFTW3 code for more than 128 cores. All other implemented options take relatively less time for execution and scale upto all the available 512 cores. With a different layout, the timing improves to some extent, as seen in table 2.

For larger 3D matrix of size $1024 \times 1024 \times 1024$, CROFT implementation with overlapping of compute and communication along with the use of single FFTW3 plan for computing 1D FFT performs better than FFTW3 and all other implemented options as seen in table 3 and figure 7.

At smaller number of cores, the difference in execution time is more (Figure 8). The CROFT implementation (option 4) is faster than FFTW3 by approx-

Number of cores	Time in (sec)				
	FFTW3	opt1	opt2	opt3	opt4
4	0.053	0.163	0.060	0.166	0.045
8	0.029	0.089	0.037	0.097	0.036
16	0.020	0.055	0.029	0.060	0.032
32	0.019	0.028	0.014	0.031	0.017
64	0.494	0.038	0.031	0.039	0.032
128	1.911	0.037	0.031	0.039	0.032
256	5.473	0.073	0.069	0.074	0.076
512	26.149	0.183	0.178	0.126	0.123

Table 1: Timings (in sec) on Param Bioblaze cluster for benchmarking with 3D matrix of size $128 \times 128 \times 128$ and nodes fill up allocation for FFTW3 and multiple options of CROFT. Opt 1: Without overlap multiple plans; Opt 2: Without overlap single plan; Opt 3: With overlap multiple plans; Opt 4: With overlap single plan

Layout (Nodes \times ppn)	Number of cores	Time in (sec)				
		FFTW3	opt1	opt2	opt3	opt4
2×2	4	0.057	0.156	0.043	0.166	0.041
4×2	8	0.032	0.079	0.025	0.082	0.021
4×4	16	0.021	0.044	0.017	0.043	0.016
4×8	32	0.019	0.027	0.013	0.039	0.029
8×8	64	0.401	0.037	0.023	0.065	0.038
8×16	128	1.911	0.037	0.031	0.039	0.032
16×16	256	5.473	0.073	0.069	0.074	0.076
32×16	512	26.149	0.183	0.178	0.126	0.123

Table 2: Timings (in sec) on Param Bioblaze cluster with processes layout.

Number of cores	Time (sec)				
	FFTW3	opt1	opt2	opt3	opt4
4	101.8044	67.1240	58.7549	61.4341	51.9448
8	51.8731	38.0646	33.8035	36.7066	29.7946
16	26.9177	25.0881	23.2374	25.8118	24.0778
32	13.3403	13.8911	12.8060	13.0762	12.1718
64	8.5792	8.1453	7.6859	7.2702	6.6610
128	5.0288	4.1973	3.9772	3.5217	3.3376
256	4.7209	2.4439	2.2346	2.1265	1.9747
512	18.8849	1.3945	1.3237	1.4165	1.2722

Table 3: Timings (in sec) on Param Bioblaze cluster for benchmarking with 3D matrix of size $1024 \times 1024 \times 1024$ with nodes fill up allocation for FFTW3 and multiple options of CROFT. Opt 1: Without overlap multiple plans; Opt 2: Without overlap single plan; Opt 3: With overlap multiple plans; Opt 4: With overlap single plan

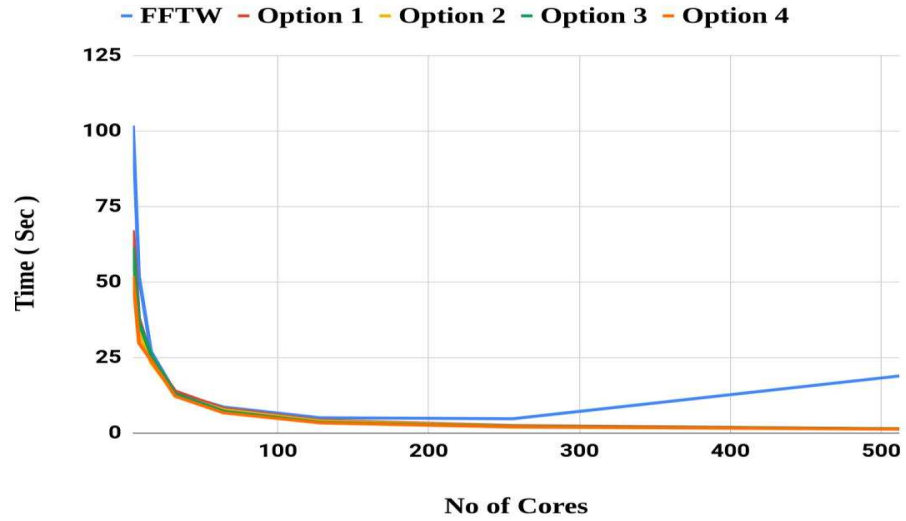


Figure 7: Comparative timing chart for data size $1024 \times 1024 \times 1024$ on Param Bioblaze cluster

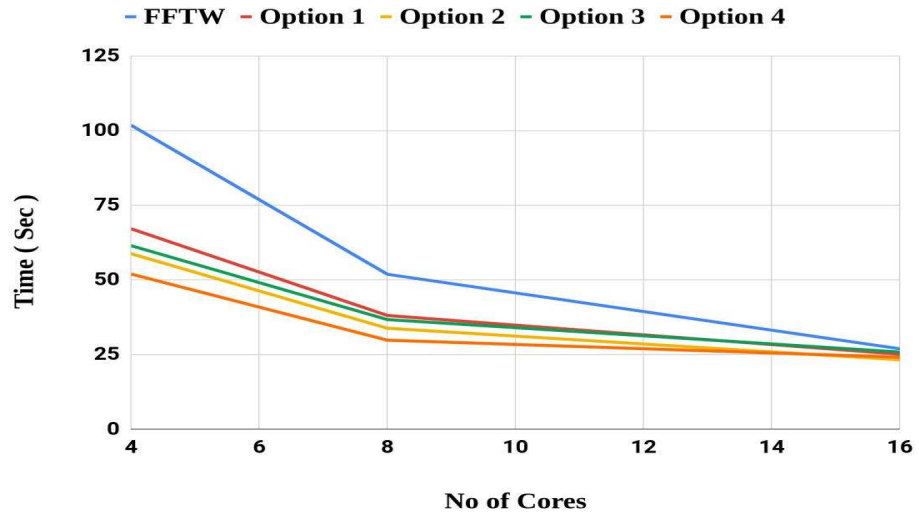


Figure 8: Timings for no of cores between 4 to 16 in figure 7

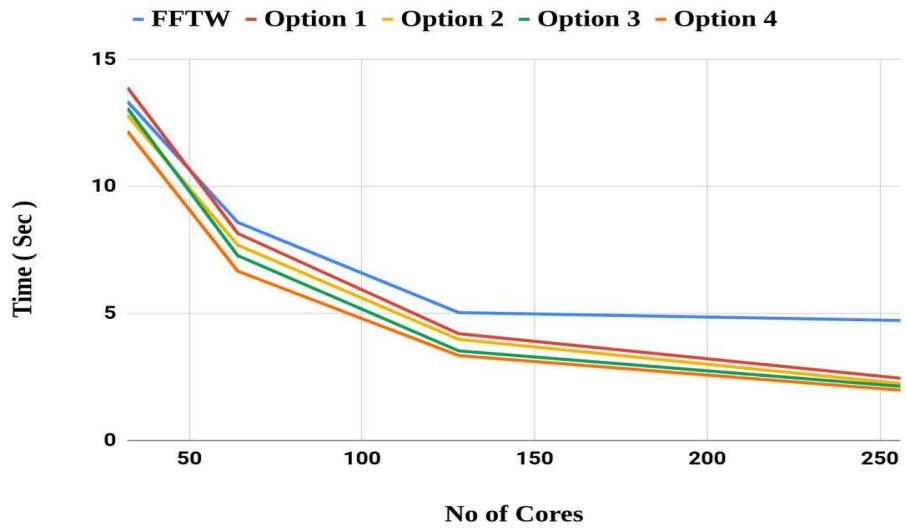


Figure 9: Timings for no of cores between 32 to 256 in figure 7

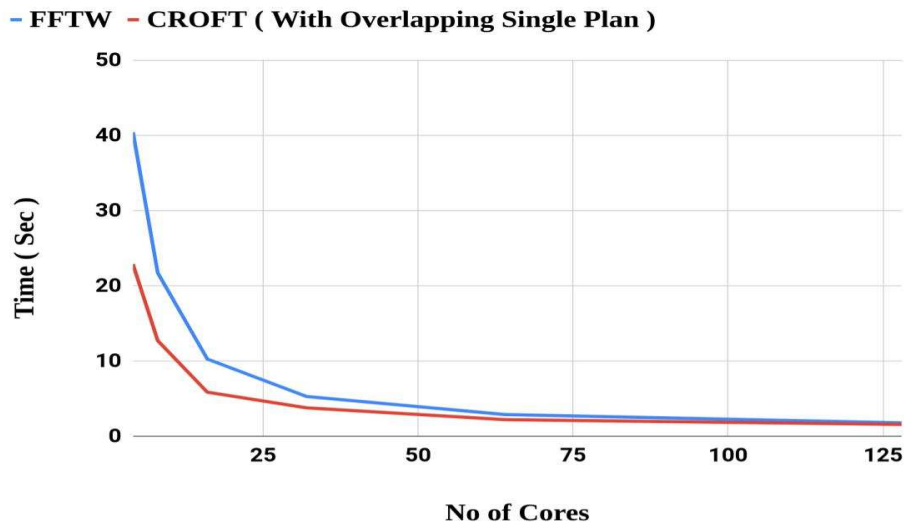


Figure 10: Comparative timing chart for data size $1024 \times 1024 \times 1024$ on Sangam Lab cluster

imately 51% when the number of cores are less (4 processes) (Figure 8) and approximately 42% when FFTW3 is having lowest time (at 256 processes) as seen in figure 9. Similar results in terms of timings have been observed in Sangam Lab cluster where, CROFT (option 4) is faster than FFTW3 as seen in figure 10.

From the scalability chart as shown in figure 11, we can see that all the implemented options of CROFT are scalable upto all the available 512 compute cores in Param Bioblaze cluster whereas performance of FFTW3 drops after 128 cores.

6.3. Profiling details

To get an insight on the difference between FFTW3 parallel 3D routines execution and CROFT execution, profiling of both the applications have been performed on 8 processes with input matrix of size $1024 \times 1024 \times 1024$. The profiling result is shown in figure 12 and 13. From the profiling data, it is clear that CROFT takes less time due to optimized user code. Inorder to produce

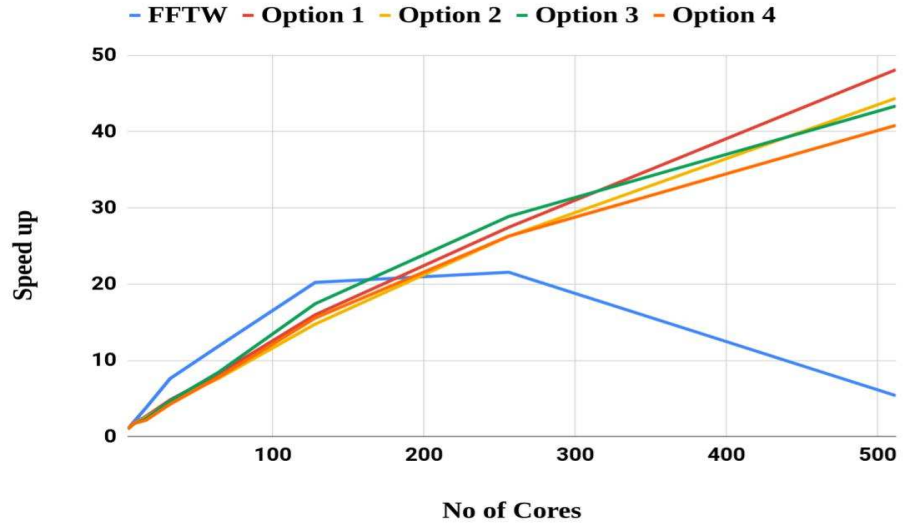


Figure 11: Speedup graph for data size 1024 x 1024 x 1024 on Param Bioblaze cluster

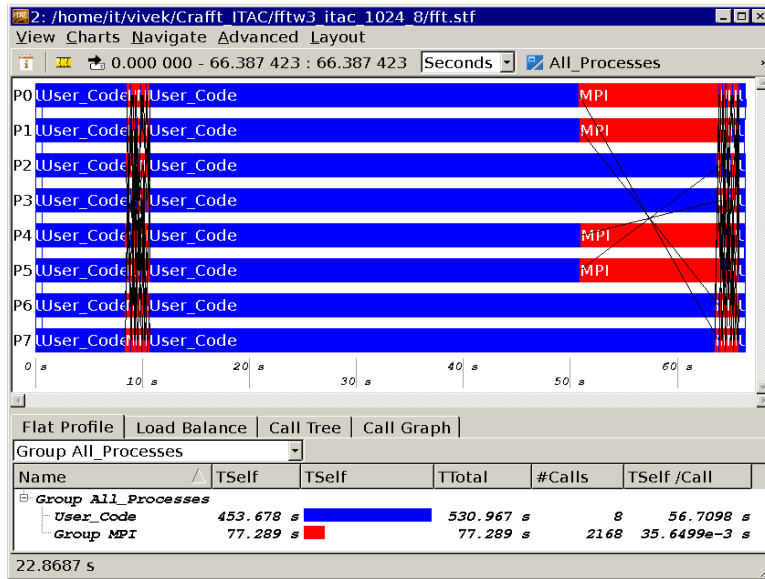


Figure 12: Event profile of fftw_mpi_plan_dft_3d API for 8 processes and input size of 1024 x 1024 x 1024 using Intel trace collector and analyzer(ITAC)

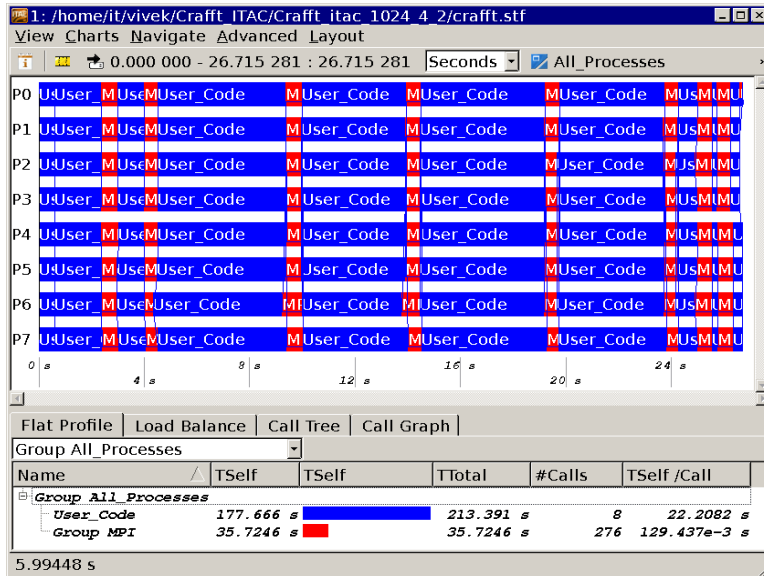


Figure 13: Event profile of croft_parallel3d API for 8 processes and input size of $1024 \times 1024 \times 1024$ using Intel trace collector and analyzer(ITAC)

the same result, FFTW3 takes 453.678 seconds for the user code to execute whereas, CROFT takes only 177.666 seconds. Similarly, MPI calls take 77.289 seconds in case of FFTW3 and 35.725 seconds in case of CROFT as seen in figure 12 and 13 respectively.

Scalability of the code may be explained by analyzing the MPI communication. The code is well load balanced with very less waiting time for MPI calls as seen in figure 13. Number of MPI calls required by FFTW3 for communication are 864 which are much more than 124 MPI calls required by CROFT. Apart from other MPI routines, there are 112 MPI_Sendrecv calls in FFTW3 routine which takes 77.136 seconds (figure 14) as compared to 64 MPI_Alltoall used in CROFT which takes 35.574 seconds (figure 15) to execute. The reduction in number of MPI communication calls in CROFT, indicated that the code is more scalable.

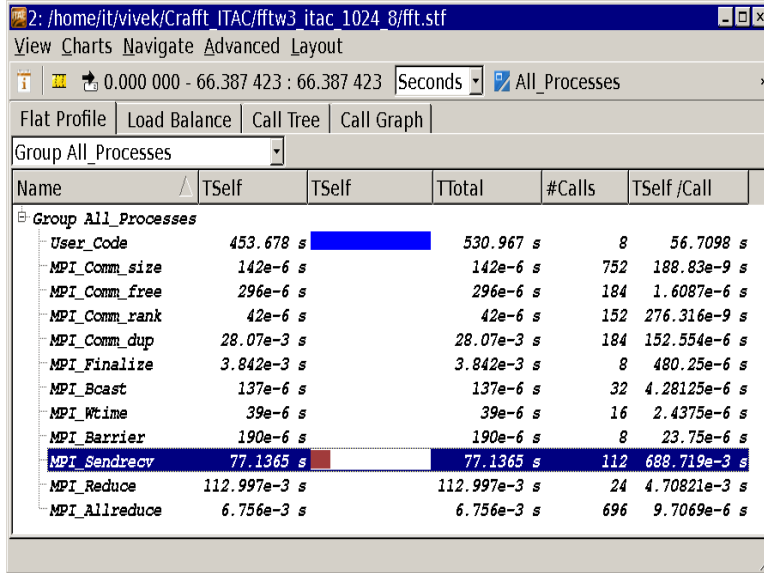


Figure 14: Function profile of fftw_mpi_plan_dft_3d API for 8 processes and input size of $1024 \times 1024 \times 1024$ using Intel trace collector and analyzer(ITAC)

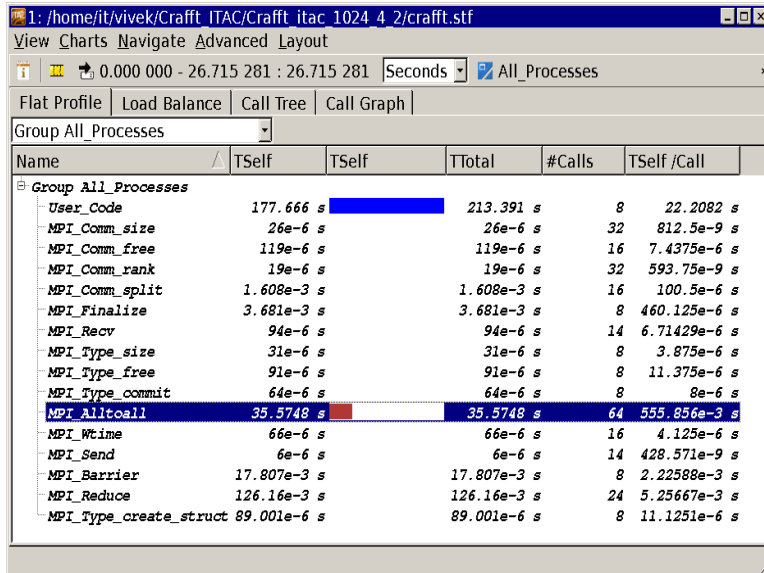


Figure 15: Function profile of croft_parallel3d API for 8 processes and input size of $1024 \times 1024 \times 1024$ using Intel trace collector and analyzer(ITAC)

7. Conclusion

For the smaller datasets, FFTW3 is faster when number of cores used are less than 32, but CROFT code implemented with option 4 (with overlap of compute and communication while using single FFTW3 plan for calculating 1D FFTs) performed better when number of cores are more than 32. For larger dataset, CROFT implementation option 4 is the best implementation with the performance improvement between 42% - 51% as seen in table 3. It also scales to more number of cores than FFTW3 due to pencil decomposition and further reducing the execution time. It can be used as one of the options for implementing exascale applications which requires 3D parallel FFT.

8. Future work

CROFT library is a pure CPU implementation and can be extended to add support for the accelerators like GPUs. Currently, CROFT uses 1D FFT from FFTW3 package, but native implementation of 1D FFT can be done as a replacement to 1D FFT from FFTW3 package, eliminating the dependency on FFTW3. CROFT is implemented for double precision complex-to-complex data only and can be further extended for implementing complex-to-real, and real-to-complex data. Moreover, there is scope for further memory optimization which can be looked at.

9. Acknowledgements

CROFT library is developed under the project National Supercomputing Mission (NSM), Government of India. The authors would like to acknowledge the use of Bioinformatics Resources and Applications Facility (BRAAF) at the Centre for Development of Advanced Computing (C-DAC), Pune and NSM Sangam Lab cluster at the Centre for Development of Advanced Computing (C-DAC), Pune for testing and benchmarking of CROFT. Authors would also like to thank Ms. Shruti Koulgi, Ms. Sunitha Manjari and Dr. Uddhavesh Sonavane for their encouragement and support.

References

- [1] S. D. Stearns, and R. A. David, *Signal Processing Algorithms*, Englewood Cliffs, NJ, Prentice Hall, 1988.
- [2] J. W. Cooley, and J. W. Tukey, An Algorithm for the Machine Calculation of Complex Fourier Series, *Mathematics of Computation*, 19, 90 (1965) 297-301. <https://doi.org/10.1090/S0025-5718-1965-0178586-1>
- [3] M. Lee, N. Malaya, and R. D. Moser, Petascale direct numerical simulation of turbulent channel flow on up to 786K cores, In *Proceedings of the International Conference on High Performance Computing, Networking, Storage and Analysis (SC '13)*, ACM, New York, USA, 61, (2013). <https://doi.org/10.1145/2503210.2503298>
- [4] R. Dror, J. P. Grossman, K. Mackenzie, B. Towles, E. Chow, J. Salmon, C. Young, J. Bank, B. Batson, M. Deneroff, J. Kuskin, R. Larson, M. Moraes, and D. Shaw, Exploiting 162-Nanosecond End-to-End Communication Latency on Anton, *ACM/IEEE International Conference for High Performance Computing, Networking, Storage and Analysis, SC 2010*, (2010) 1-12. <https://doi.org/10.1109/SC.2010.23>.
- [5] S. Aarseth, *Gravitational N-Body Simulations: Tools and Algorithms* (Cambridge Monographs on Mathematical Physics), Cambridge: Cambridge University Press, 2003. <https://doi.org/10.1017/CBO9780511535246>
- [6] O. Bruno, and L. Kunyansky, A Fast High-Order Algorithm for the Solution of Surface Scattering Problems: Basic Implementation, Tests, and Applications, *Journal of Computational Physics*, 169, (2001) 80-110. <http://doi.org/10.1006/jcph.2001.6714>.
- [7] J. R. Phillips, and J. K. White, A precorrected-FFT method for electrostatic analysis of complicated 3-D structures, *Transactions on Computer-Aided Design of Integrated Circuit Systems*, 16, 10 (2006), 1059-1072. <http://dx.doi.org/10.1109/43.662670>

- [8] I. T. Foster, and P. H. Worley, Parallel Algorithms for the Spectral Transform Method, *SIAM Journal on Scientific Computing*, 18, 3 (1997), 806-837. <https://doi.org/10.1137/S1064827594266891>
- [9] V. Kumar, A. Grama, A. Gupta, and G. Karypis, *Introduction to Parallel Computing: Design and Analysis of Algorithms*, Benjamin-Cummings Publ. Co., Inc., Redwood City, CA, USA, 1994.
- [10] A. Bueno-Orovio, V. M. Prez-Garca, and F. H. Fenton, Spectral Methods for Partial Differential Equations in Irregular Domains: The Spectral Smoothed Boundary Method, *SIAM Journal on Scientific Computing*, 28, 3 (2006) 886-900. <https://doi.org/10.1137/040607575>
- [11] M. Frigo, and S. G. Johnson, The Design and Implementation of FFTW3, *Proceedings of the IEEE*, 93, (2005) 216-231. <https://doi.org/10.1109/JPROC.2004.840301>
- [12] M. Pippig, PFFT: An Extension of FFTW to Massively Parallel Architectures, *SIAM Journal on Scientific Computing*, 35, (2013). <http://doi.org/10.1137/120885887>
- [13] D. Pekurovsky, P3DFFT: A Framework for Parallel Computations of Fourier Transforms in Three Dimensions, *SIAM Journal on Scientific Computing*, 34, 4 (2012) 192-209. <https://doi.org/10.1137/11082748X>
- [14] E. J. Bylaska, M. Valiev, R. Kawai, and J. H. Weare, Parallel implementation of the projector augmented plane wave method for charged systems, *Computer Physics Communications*, 143, 1 (2002) 11-28. [https://doi.org/10.1016/S0010-4655\(01\)00413-1](https://doi.org/10.1016/S0010-4655(01)00413-1).
- [15] A. Gholami, J. Hill, D. Malhotra, and G. Biros, AccFFT: A library for distributed-memory FFT on CPU and GPU architectures, (2015). arXiv, [abs/1506.07933](https://arxiv.org/abs/1506.07933).
- [16] U. Nidhi, K. Paul, A. Hemani, and A. Kumar, High performance 3D-FFT implementation, *IEEE International Symposium*

- on Circuits and Systems (ISCAS), Beijing, 201, (2013) 2227-2230.
<https://doi.org/10.1109/ISCAS.2013.6572319>
- [17] J. Sheng, B. Humphries, H. Zhang, and M. C. Herbordt, Design of 3D FFTs with FPGA clusters, IEEE High Performance Extreme Computing Conference (HPEC), Waltham, MA, (2014) 1-6.
<https://doi.org/10.1109/HPEC.2014.7040997>
- [18] S. Keskin, E. Erdil, and T. Koak, An efficient parallel implementation of 3D-FFT on GPU, IEEE High Performance Extreme Computing Conference, Waltham (2017).
- [19] S. Song, and J. K. Hollingsworth, Scaling Parallel 3-D FFT with Non-Blocking MPI Collectives, 5th Workshop on Latest Advances in Scalable Algorithms for Large-Scale Systems, New Orleans, LA, (2014) 1-8.
<https://doi.org/10.1109/ScalA.2014.9>
- [20] V. Nikl, and J. Jaros, Parallelisation of the 3D Fast Fourier Transform Using the Hybrid OpenMP/MPI Decomposition. In: Hlinn P. et al. (eds) Mathematical and Engineering Methods in Computer Science, Lecture Notes in Computer Science, 8934. Springer, Cham 2014.
- [21] U. Sigrist, Optimizing parallel 3D fast Fourier transformations for a cluster of IBM POWER5 SMP nodes, PhD thesis, The University of Edinburgh, 2007.
- [22] M. Frigo, A fast Fourier transform compiler, Proceedings of the ACM SIGPLAN 1999 conference on Programming language design and implementation (PLDI '99), ACM, New York, NY, USA, (1999) 169-180.
<https://dx.doi.org/10.1145/301618.301661>
- [23] N. Li, and S. Laizet, 2DECOMP&FFT A highly scalable 2D decomposition library and FFT interface, Cray User Group 2010 conference, Edinburgh, (2010).

- [24] O. Ayala, L. P. Wang, Parallel implementation and scalability analysis of 3D Fast Fourier Transform using 2D domain decomposition, *Parallel Computing*, 39, 1, (2013) 58-77. <https://doi.org/10.1016/j.parco.2012.12.002>.
- [25] S. G. Sedukhin, Co-design of Extremely Scalable Algorithms/Architecture for 3-Dimensional Linear Transforms, Technical Report TR2012-001, The University of Aizu, (2012).
- [26] <http://www.fftw.org/>
- [27] <https://www.p3dfft.net/>
- [28] http://www.gromacs.org/Documentation/-Installation_Instructions_5.0?highlight=ffts#fast-fourier-transfor